haematologica
Journal of the Ferrata Storti Foundation

Metabolic profile evolution in relapsed/refractory B-cell non-Hodgkin lymphoma patients treated with CD19 chimeric antigen receptor T-cell therapy and implications in clinical outcome

by Serena De Matteis, Laura Del Coco, Federica De Castro, Anna Maria Giudetti, Beatrice Casadei, Francesco Iannotta, Francesco De Felice, Enrica Tomassini, Francesca Vaglio, Maria Naddeo, Irene Salamon, Gianluca Storci, Noemi Laprovitera, Daria Messelodi, Salvatore Nicola Bertuccio, Marta Tassoni, Barbara Sinigaglia, Francesco Barbato, Margherita Ursi, Elena Campanini, Enrico Maffini, Marcello Roberto, Cinzia Pellegrini, Elisa Dan, Chiara Pirazzini, Paolo Garagnani, Manuela Ferracin, Pier Luigi Zinzani, Francesco Paolo Fanizzi, Massimiliano Bonafè and Francesca Bonifazi

Received: February 27, 2024.
Accepted: December 11, 2024.

Citation: Serena De Matteis, Laura Del Coco, Federica De Castro, Anna Maria Giudetti, Beatrice Casadei, Francesco Iannotta, Francesco De Felice, Enrica Tomassini, Francesca Vaglio, Maria Naddeo, Irene Salamon, Gianluca Storci, Noemi Laprovitera, Daria Messelodi, Salvatore Nicola Bertuccio, Marta Tassoni, Barbara Sinigaglia, Francesco Barbato, Margherita Ursi, Elena Campanini, Enrico Maffini, Marcello Roberto, Cinzia Pellegrini, Elisa Dan, Chiara Pirazzini, Paolo Garagnani, Manuela Ferracin, Pier Luigi Zinzani, Francesco Paolo Fanizzi, Massimiliano Bonafè and Francesca Bonifazi. Metabolic profile evolution in relapsed/refractory B-cell non-Hodgkin lymphoma patients treated with CD19 chimeric antigen receptor T-cell therapy and implications in clinical outcome.
Haematologica. 2024 Dec 19. doi: 10.3324/haematol.2024.285154 [Epub ahead of print]

Metabolic profile evolution in relapsed/refractory B-cell non-Hodgkin lymphoma patients treated with CD19 chimeric antigen receptor T-cell therapy and implications in clinical outcome

Serena De Matteis[1*], Laura Del Coco[2*], Federica De Castro[2], Anna Maria Giudetti[2], Beatrice Casadei[1], Francesco Iannotta[1], Francesco De Felice[1,3], Enrica Tomassini[1], Francesca Vaglio[1,3], Maria Naddeo[1], Irene Salamon[1], Gianluca Storci[1], Noemi Laprovitera[1], Daria Messelodi[1], Salvatore Nicola Bertuccio[1], Marta Tassoni[3], Barbara Sinigaglia[1], Francesco Barbato[1,3], Margherita Ursi[1,3], Elena Campanini[1], Enrico Maffini[1], Marcello Roberto[1,3], Cinzia Pellegrini[1], Elisa Dan[1], Chiara Pirazzini[3], Paolo Garagnani[1,3], Manuela Ferracin[1,3], Pier Luigi Zinzani[1,3], Francesco Paolo Fanizzi[2§], Massimiliano Bonafè[1,3§], Francesca Bonifazi[1]

[1]IRCCS Azienda Ospedaliero-Universitaria di Bologna, Bologna Italy; [2]Department of Biological and Environmental Sciences and Technologies (Di.S.Te.B.A.), University of Salento, Lecce, Italy. [3]Department of Medical and Surgical Sciences (DIMEC) University of Bologna, Bologna, Italy.

Running head: Metabolic evolution in CAR-T-treated patients

SDM and LDC equally contributed as co-first authors.

Corresponding author: Massimiliano Bonafè, IRCCS Azienda Ospedaliero-Universitaria di Bologna and Department of Medical and Surgical Sciences (DIMEC) University of Bologna, Bologna, Italy. massimiliano.bonafe@unibo.it

Co-corresponding: Francesco Paolo Fanizzi, Department of Biological and Environmental Sciences and Technologies (Di.S.Te.B.A.), University of Salento, Lecce, Italy. fp.fanizzi@unisalento.it

Data-sharing statement. This study is available at the NIH Common Fund's National Metabolomics Data Repository (NMDR) website https://www.metabolomicsworkbench.org where

it has been assigned Study ID ST003205. The data can be accessed directly via its Project DOI: http://dx.doi.org/10.21228/M8G143.

AUTHOR CONTRIBUTIONS

SDM, MB, and FB designed the study. BC, FDF, ET, FB, MU, EM, MR, CP, PLZ and FB contributed patient samples and clinical data. SDM, LDC, FDC, AMG, FI, FV, MN, IS, GS, NL, DM, SNB, MT, BS, EC, MF, FPF, MB conducted the experiments and analyzed the data. SDM, LDC, AMG, MB and FB wrote the article. SDM, FDC, AMG, CP, PG, MB revised the manuscript. All authors read and agreed to the final version of the article.

DISCLOSURES

P.L.Z: scientific advisory boards: Secura Bio BIO, Celltrion, Gilead, Janssen-Cilag, BMS, Servier, Sandoz, MSD, TG Therap., Takeda, Roche, EUSA Pharma, Kiowa Kirin, Novartis, ADC Therap., Incyte, Beigene; consultancy: EUSA Pharma, MSD, Novartis; speaker's bureau: Celltrion, Gilead, Janssen-Cilag, BMS, Servier, MSD, TG Therap., Takeda, Roche, EUSA Pharma, Kiowa Kirin, Novartis, Incyte, Beigene.

M.B: Research Grant from NEOVII.

F.B: advisory boards and speaker fees: NEOVII, NOVARTIS, KITE, GILEAD, PFIZER, CELGENE, MSD, SANOFI, JAZZ Pharmaceuticals, BMS.

The remaining authors declare that the research was conducted in the absence of any commercial or financial relationships that could be construed as a potential conflict of interest.

Word count abstract: 192

Word count main text: 2870

Tables: 1

Figures: 5

Supplementary Figures: 4

Supplementary Tables: 4

ClinicalTrials.gov identifier: NCT04892433

ACKNOWLEDGEMENTS. The authors thank AIL Bologna ODV, the Italian Association for Research on Leukemia, lymphoma and myeloma for the support of the Laboratory of Immunobiology of Transplant and Cellular Therapies, IRCCS AOU di Bologna, Bologna, Italy. Francesca Bonifazi, MD, PhD

FUNDING. The work was funded to FB by the Italian Ministry of Health, RC-2023-2778976 for the article processing charge and consumables and Italian Ministry of University: Heal Italia health extended alliance for innovative therapies, advanced lab-research, and integrated approaches of precision medicine (code PE0000019) for consumables.

Abstract

Plasma metabolomics analysis was performed on 44 patients with relapsed/refractory B-cell non-Hodgkin lymphoma (r/r/B-NHL) infused with approved CD19.CAR-T cell products at the time of pre-lymphodepletion (PLD) and at day +1, +7, and +30 after CAR-T cell infusion. At the PLD time point, a metabolic profile characterized by high lipoproteins and lactate and low glucose contributed to poor outcome prediction in association with high lactate dehydrogenase levels. At day+1, higher plasma levels of lipid metabolism products and lower glucose and glycoproteins levels were observed in tisa-cel compared to axi-cel-treated patients.

At day+30, discriminant analysis found two clusters in a subgroup of patients, one with CR lasting one year after therapy, and another who relapsed within one year (relapsed>D30). This latter showed a higher content of N-GlycA, a known biomarker of systemic inflammation that is also correlated with C-reactive protein in our case setting of relapsing patients. Our data show complex metabolomic changes that track the evolution of the disease and drug activity in the first 30 days of CAR-T cell therapy. Conceivably, a pro-inflammatory drift may be linked to a forthcoming disease relapse in CAR-T patients.

Keywords: CAR-T cell therapy; lymphoma; metabolomics; inflammation.

INTRODUCTION

Chimeric antigen receptor (CAR)-T cell therapy is an innovative approach for patients affected by relapsed or refractory aggressive B-cell non-Hodgkin lymphoma (r/r B-NHL) who either failed to respond to autologous stem cell transplantation or are ineligible for it.[1] Some pretreatment factors have been identified to be associated with relapse or progression, such as elevated lactate dehydrogenase (LDH),[2] tumor burden measured either by the lesion diameter or by the total metabolic tumor volume on positron emission tomography and computed tomography (PET)-CT scan, and more than one extranodal sites involved.[3] Our study aims to investigate the potential clinical utility of a Nuclear Magnetic Resonance (NMR)-based metabolomic approach to differentiate patients who achieve a durable response to CAR-T cell therapy from those who do not respond or progress after an early metabolic response at 1-month after CAR-T cell therapy. In this real-life study, plasma samples of 44 r/r B-NHL patients treated with AIFA-approved CD19.CAR-T cell products were analyzed with a metabolomic approach based on NMR spectroscopy at pre-lymphodepletion (PLD) and after infusion.

METHODS

Patients

This is a prospective observational tissue study performed in patients affected by r/r B-NHL after CD19.CAR-T cell therapy with axi-cel and tisa-cel. Only patients with diffuse large B□cell lymphoma (DLBCL), DLBCL transformed from follicular lymphoma (tFL), high-grade B-cell lymphoma (HGBCL), and primary mediastinal B□cell lymphoma (PMBCL) were included. Cytokine release syndrome (CRS) and immune effector cell□associated neurotoxicity syndrome (ICANS) were graded according to the American Society for Transplantation and Cellular Therapy (ASCT) criteria.[4] All eligible patients were treated at IRCCS AOU di Bologna, after signing a written informed consent. The study was approved by the local Ethical Committee in agreement with the Helsinki Declaration and registered at clinicaltrial.gov NCT04892433.

Sample collection and assessment of biochemical parameters

Blood samples were collected at the PLD time point and day +1 (D1), +7 (D7), and +30 (D30) after CAR-T cell infusion, when available. Plasma separation was performed within 4 hours after blood sample collection by centrifugation at 1000xg for 15 minutes at room temperature. Plasma aliquots were collected and stored at -80°C. All the serum biochemistry reported in the study was assessed according to the standard practice at the IRCCS AOU Bologna analysis service.

NMR measurements and data processing

The present research follows the requirements and recommendations for the handling and processing of blood plasma for metabolomics analysis in the pre-examination processes according to ISO 23118:2021. We performed a study assessing the compliance of the datasets in the Metabolomics Workbench repository[5]. In **Supplementary Methods,** plasma sample preparation for NMR measurements is reported.

Statistical analysis

Unsupervised principal component analysis (PCA), and supervised orthogonal partial least squares discriminant analysis (OPLS-DA) were performed on NMR data using Simca 14.0 software (SIMCA® https://www.sartorius.com/en). For all the statistical models performed on NMR data, the goodness-of-fit (R^2X), the proportion of the variance that is explained by the model (R^2Y), and the goodness-of-prediction of the model (Q^2) parameters were evaluated, providing reliability and an internal measure of consistency between the original and (7-fold) cross-validated predicted data.[6] Moreover, for OPLS-DA models, Variable importance for projection (VIP) and loadings vectors scaled as correlation poso(corr) are also considered for discriminating variables.[7] Both univariate and multivariate statistical analyses were performed using MetaboAnalyst software[8] and the SPSS/PC-computer program (SPSS, Chicago, IL, USA).

Summary statistics of all explanatory variables are reported for the whole population as required. Association between PC1 and PC2 obtained at the PLD time point and patients' features included in

Table 1 was represented using boxplots and analyzed by Kruskal-Wallis tests, with Bonferroni correction for multiple comparisons. Statistical significance was set at $p \leq 0.05$. Given the presence of outliers and the non-normality of the data, correlation is measured by Spearman's coefficient. All variables significantly associated with clinical outcomes were evaluated in a multiple Cox regression. In particular, stepwise methods with 0.1 significance level including all covariates were performed to select the best subset of predictors. Finally, predictive performance of the model was measured according to the resulting operating characteristic (ROC) area under the curve (AUC).

RESULTS

Patient characteristics

All patients (n=44, **Table 1**) had r/r B-NHL: thirty-six (81.9%) DLBCL (including fifteen tFL), six (13.6%) PMBCL and two patients (4.5%) with HGBCL. Twenty-four patients (55%) received axi-cel and twenty (45%) received tisa-cel after a median of three prior lines of treatment. The average age was 60 years (range 21-70). All patients underwent CAR-T cell infusion following standard lymphodepletion chemotherapy with cyclophosphamide (250-500 mg/m2) and fludarabine (25-30 mg/m2) administered intravenously on days -5, -4, and -3 according to standard practice. Among forty-four patients who underwent infusion, thirty-eight (86.4%) developed CRS (any grade). Four patients (9.1%) experienced grade ≥ 3 CRS. Within 1-month of CD19.CAR-T cell infusion, fourteen (32%) of forty-four patients developed ICANS of any grade. Six patients (13.6%) developed ICANS grade ≥3. Two patients (4.5%) died of fatal neurotoxicity with diffuse cerebral edema (ICANS, grade 5). At one-month post-infusion, the overall response rate (ORR) was 64%: fourteen (32%) patients achieved complete remission (CR), and fourteen (32%) patients achieved partial remission (PR); eight (18%) patients achieved progressive disease (PD) and six (14%) had stable disease (SD). At the latest available follow□up (1-year), thirteen patients were in CR and three in PR. The others (n=26) had experienced progression during the course of follow-up.

Median follow-up was 364 days for overall survival (OS) and 147 days for time-to-progression (TTP) and progression-free survival (PFS).

Metabolic profile of r/r B-NHL patients before and after receiving CAR-T cell therapy

We performed a PLD metabolomic profile of 44 patients of whom 22 also at D1, D7 and D30 time points after CAR-T cell infusion (**Supplementary Methods and Figure S1A).**

A representative ^{1}H NMR spectrum and the chemical shifts (δ) and assignments of metabolites resonances of the acquired ^{1}H NMR spectra are provided in **Supplementary Methods** and **Figure S1B** and in **Table S1**.

Firstly, we focused on pre-treatment metabolic profile and the PCA model was built using the first two principal components (PC) that explained 34.6% and 11.7% of the total variance in an eight-components model (**Supplementary Figure S2A**). NMR signals related to lipoproteins and glucose were found at positive and negative values of the first PC1 component, respectively (**Supplementary Figure S2B**). Moreover, the contribution of loadings related to lactate and glycoproteins, specifically N-GlycA which refers to a subset of glycan N-acetylglucosamine residues (NMR signal at 2.05 ppm, related to -$COCH_3$ acetyl groups of sera glycoproteins), were both found at positive values of PC2 (**Supplementary Figure S2B**).

We performed the Kruskal–Wallis multiple comparisons between the first two PC and anthropometric and clinical parameters included in **Table 1.**

As reported in **Figure 1,** the PLD metabolic profile described by PC1 was different according to diagnosis ($p=0.039$). We also explored the potential correlation with variables associated with inflammatory status and/or tumor burden, namely triglycerides, LDH, fibrinogen, ferritin, and C-reactive protein (CRP) measured at PLD (**Figure 2A**). PC1 was positively correlated with triglycerides ($r=0.81$, $p<0.001$) (**Figure 2A**).

Cox regression was then used in TTP to determine the influence of multiple variables on the outcome. Starting with the whole set of covariates, stepwise selection methods on the whole set of

patients identified PC1 (HR=1.052, 95% CI, p=0.01) and LDH (HR=1.001, 95% CI, p=0.03) as predictors. The resulting Cox model confirmed the predictive power of PC1 since its addition into the model gave better predictions in terms of ROC-AUC with respect to the model with LDH alone (AUC_{LDH}-=0.61 and $AUC_{-LDH+PC1}$-=0.81, respectively, **Figure 2B**).

Based on the contribution of the loadings for the first two PC (see **Supplementary Figure S2B**), the box-whisker plots report the distribution of discriminant metabolites according to the last available follow-up (CR, n=13 vs PD, n=26 vs PR, n=3, **Supplementary Figure S2C)**. Specifically, we observed higher levels of lipoproteins and lactate and lower amounts of N-GlycA, succinate and glucose in PD and PR patients than in CR ones (**Supplementary Figure S2C).**

A supervised analysis (OPLS-DA) showed a good separation between the most representative patient's groups (CR, n=13 *vs* PD, n=26, **Figure 2C**). The most evident differences in metabolites between the patient groups were observed in the levels of lipoproteins/lipids and lactate, which were higher in PD than CR, as well as in the level of glucose, which was lower in PD than CR (**Figure 2D and Table S2**).

Next, we focused on a sub-cohort of twenty-two patients whose plasma samples were available to test differences in the metabolomic profiles across time after CAR-T infusion (D1, D7, and D30) (**Figures 3A, C, and D**) according to the infused product (axi-cel vs tisa-cel). No differences in the metabolic profile at the PLD time point were observed **(Supplementary Figure S3)**, but specific metabolic signatures were identified among patients, specifically at D1 (**Figure 3A).** These differences progressively disappeared over time **(Figures 3C and D).** As reported in **Figure 3B and Table S3**, at D1, the S-line plot showed higher levels of lipoproteins, 3-hydroxybutyrate (3-OH butyrate), and acetate, and lower levels of glucose and GlycA, which refers to a subset of glycan N-acetylglucosamine residues in tisa-cel-treated patients compared to those infused with axi-cel.

Moreover, time-dependent metabolic changes were observed from D1 to D30 in patients stratified according to the last available follow-up (**Figure 4**). Specifically, a reduced N-GlyA and lipoproteins/lipids content was observed in patients who achieved CR (**Figure 4A and B**) compared

with PD patients who showed an increased content of succinate/pyruvate and lactate (**Figure 4C and D**). This observation suggests that plasma can efficiently mirror the metabolic pattern of lymphoma cells that survive within 30 days after CAR-T therapy.

Considering this finding, we considered a subgroup of patients in whom PET/TC scans showed a CR/PR (n=14) at D30 time point. Discriminant analysis found two clusters of patients, one with CR lasting one year after therapy (stable CR>D30), and another who relapsed within one year (relapsed>D30) (**Figure 5A**). Metabolic differences in the content of N-GlycA, histidine, glutamate, phenylalanine and branched-chain amino acids (BCAA) (leucine, isoleucine and valine) were observed between relapsed>D30 and stable CR>D30 (**Figure 5B, 5C and Table 4**). The unpaired t-test analysis showed that N-GlycA and histidine were significantly enriched in relapsed>D30 patients (**Figure 5C and D and Table S4**). Moreover, a correlation between N-GlycA and CRP was found in the case set of relapsing patients (spearman rho=.93**).

To further prove that glycans are associated with poor prognosis in the post-CAR-T infusion setting, we took advantage of a DSA-FACE-based method (**Supplementary Methods**) for glycans assessment[9]. The assay allowed us to detect a subset of eight N-glycans on D30 plasma samples from an independent cohort of 20 patients who were in CR/PR on the basis of the D30 PET/TC scans. This approach gave us the possibility to calculate the GlycoAge[10] score which, in our case series, was positively correlated with CRP (rho=0.58, p=0.01) and that showed a trend towards higher levels (p=0.076) in patients who relapsed at 3- or 6-months compared to those who remained in CR up to 6-months (**Supplementary Fig. S4)**.

Discussion

Due to the high morbidity and financial costs associated with CAR-T cell therapy, it is important to identify robust biomarkers predictive of either responsiveness or resistance to treatment.

In previous studies, analysis of several biomarkers identified a significant decrease in overall survival in patients with elevated LDH levels in the circulation, measured both before

lymphodepletion and at the time of cell infusion.[3,11,12] Results from the US lymphoma CAR-T consortium evaluating axi-cel outcomes reported higher plasma levels of LDH before conditioning to be a significant predictor of lower OS.[3] Moreover, multivariate analysis of tisa-cel clinical trial reported that patients with elevated pre-CAR-T LDH levels had poorer performance-free survival and OS.[11]

In this real-life study, a metabolomic approach based on NMR spectroscopy was performed on plasma samples obtained from r/r B-NHL patients treated with CD19.CAR-T cell therapy at the PLD time point and D1, D7 and D30 after infusion.

Interestingly, at the PLD time point, a metabolic profile characterized by high lipoproteins and lactate and low glucose improved the capability of high LDH levels to predict a poor outcome. Indeed, the same metabolic profile has been observed in patients who progress or lose CAR-T response compared to those achieving complete remission within 1-year. Bearing in mind that cancer cells derive most of their energy from aerobic glycolysis, with the production of lactate (Warburg Effect), the metabolic profile of these patients recapitulates this effect. Moreover, we can hypothesize that the high level of lipoproteins in patients who will progress or lose the response to CAR-T cell therapy could be involved in disease progression and resistance to treatment. Indeed, recent literature reports that elevated levels of cholesterol and lipids increase oxidative stress,[13] and impair T-cell immune response.[14]

In a subgroup of patients, we described the effect of the infused CAR-T cell products on the metabolic profile. Patients treated with tisa-cel showed higher plasma levels of lipid metabolism products while those treated with axi-cel showed higher levels of glucose and glycoproteins. This result could be attributable to the different co-stimulatory domains of the two CAR-T cell products. I*n vitro* and i*n vivo* studies have reported that 4-1BB co-stimulatory domain induces in CAR-T cells a shift of metabolism towards fatty acid beta-oxidation, while CD28 domain increases glycolytic metabolism.[15,16]

According to the last available follow-up, a time-dependent change in metabolome was observed from D1 to D30. PD patients were characterized by higher lactate and pyruvate/succinate at D30 after CAR-T cell infusion. Lactate, which is produced by glucose fermentation and released from the cells into the surrounding medium, is considered an immunosuppressive metabolite as it promotes tumor progression, induces angiogenesis, stimulates amino acid metabolism, inhibits cytotoxic T, NK, and DC cells, and prevents antitumor response.[17] The higher level of lactate found in PD patients, as compared to those in CR/PR, could be related to the worsening of the patient's condition at D30 after infusion. It is known that tumor cells have a glycolytic/fermentative metabolism, consume large quantities of glucose, but produce lactate even in the presence of oxygen. In the tumor microenvironment (TME), a large amount of lactate accumulation can lead to immunosuppression via M2-like tumor-associated macrophage polarization[18,19] and myeloid-derived suppressor cells (MDSC) expansion that inhibits NK cell-mediated cytotoxic activity.[20] Moreover, an inhibitory effect of lactic acid on T cell fitness has been suggested by Fisher K et al, who showed that lactic acid suppressed proliferation and cytokine production of human cytotoxic T lymphocytes, leading to a cytotoxic activity reduction[21]. Furthermore, an increase in lactic acid was found in acute myeloid leukemia (AML) patients relapsed after allogeneic-hematopoietic cell transplantation[22]. Noteworthy, the authors showed that lactic acid released by AML cells reduced glycolytic activity of T cells and led to their metabolic and proliferative dysfunction[22].

PET-CT scan better describes the response to CAR-T cell therapy and the first evaluation is assessed at D30 after infusion. However, interpretation of the data can be complicated due to confounding factors related to cytotoxic effects induced by CAR-T cells. Considering the metabolomic profile of patients with early CR/PR assessed by PET/CT at D30 time point, those who lost response at 90 or 180 days had a higher content of N-GlycA and histidine, compared to patients who remained in CR for up to 1 year. Emerging studies revealed that altered amino acid metabolism is linked to tumor growth, immunosuppression, and therapeutic resistance through the regulation of immune cell fate.[23] Noteworthy, via the action of histidine decarboxylase, that is

found in cells belonging to the myeloid and lymphoid lineage, histidine forms histamine, a crucial player of inflammation[24,25]. Notably, N-GlycA is a biomarker of systemic inflammation[26,27] which correlates with circulating inflammatory proteins (e.g IL-6, tumor necrosis factor-α, fibrinogen, CRP) that are known to be associated with adverse outcome in CAR-T therapy[28]. In line with this tenet, a high correlation between N-GlycA and CRP was found in the case set of relapsing patients.

According to the data showing that protein glycation increases in presence of chronic inflammation[10,29], and that is increased in cancer bearing patients[30], a trend towards higher GlycoAge score was found in an independent cohort of patients who relapsed at 3- or 6-months (relapsed>D30) compared to those who remained in CR for up to 6-months (CR>30).

As both NMR-detected N-GlycA and the GlycoAge[11] score are positively correlated with CRP, our data support the notion that a search for sensitive markers of cancer-related pro-inflammatory drift[30] is likely to be useful in the CAR-T patients' follow-up. Though the limited sample size of our study provides only a starting point that needs to be validated in larger future studies, circulating metabolites related to systemic inflammation are likely to be important biomarkers of CAR-T cell response.

REFERENCES

1. Crump M, Neelapu SS, Farooq U, et al. Outcomes in refractory diffuse large B-cell lymphoma: results from the international SCHOLAR-1 study. Blood. 2017;130(16):1800-1808.
2. Locke FL, Rossi JM, Neelapu SS, et al. Tumor burden, inflammation, and product attributes determine outcomes of axicabtagene ciloleucel in large B-cell lymphoma. Blood Adv. 2020;4(19):4898-4911.
3. Nastoupil LJ, Jain MD, Feng L, et al. Standard-of-care axicabtagene ciloleucel for relapsed or refractory large B-cell lymphoma: results from the US Lymphoma CAR T Consortium. J Clin Oncol. 2020;38(27):3119-3128.
4. Lee DW, Santomasso BD, Locke FL, et al. ASTCT consensus grading for cytokine release syndrome and neurologic toxicity associated with immune effector cells. Biol Blood Marrow Transplant. 2019;25(4):625-638.
5. Sud M, Fahy E, Cotter D et al. Metabolomics Workbench: An International Repository for Metabolomics Data and Metadata, Metabolite Standards, Protocols, Tutorials and Training, and Analysis Tools. Nucleic Acids Res. 2016;44(D1):D463-470.
6. Girelli CR, Del Coco L, Papadia P, De Pascali SA, Fanizzi FP. Harvest year effects on Apulian EVOOs evaluated by ^{1}H NMR based metabolomics. PeerJ. 2016;4:e2740.
7. Del Coco L, Felline S, Girelli CR, et al. ^{1}H NMR Spectroscopy and MVA to evaluate the effects of caulerpin-based diet on Diplodus sargus lipid profiles. Mar Drugs. 2018;16(10):390.
8. Chong J, Soufan O, Li C, et al. MetaboAnalyst 4.0: Towards more transparent and integrative metabolomics analysis. Nucl Acids Res. 2018;46(W1):W486-W494.
9. Vanhooren V, Laroy W, Libert C, Chen C. N-glycans profiling in the study of human aging. Biogerontology. 2008; 9(5):351-356.

10. Vanhooren V, Dewaele S, Libert C, et al. Serum N-glycan profile shift during human ageing. Exp. Gerontol. 2010; 45(10):738-743.
11. Westin JR, Tam CS, Borchmann P, et al. Correlative analyses of patient and clinical characteristics associated with efficacy in tisagenlecleucel-treated relapsed/refractory diffuse large B-cell lymphoma patients in the Juliet trial. Blood. 2019;134(Supplement_1):4103.
12. Detroit M, Collier M, Beeker N, et al. Predictive Factors of Response to Immunotherapy in Lymphomas: A Multicentre Clinical Data Warehouse Study (PRONOSTIM). Cancers (Basel). 2023;15(16):4028.
13. Lu J, Mitra S, Wang X, Khaidakov M, Mehta JL. Oxidative stress and lectin-like ox-LDL receptor LOX- 1 in atherogenesis and tumorigenesis. Antioxid Redox Signal. 2011;15(8):2301-2333.
14. Khojandi N, Kuehm LM, Piening A, et al. Oxidized Lipoproteins Promote Resistance to Cancer Immunotherapy Independent of Patient Obesity. Cancer Immunol Res. 2021;9(2):214-226.
15. Kawalekar OU, O'Connor RS, Fraietta JA, et al. Distinct Signaling of Coreceptors Regulates Specific Metabolism Pathways and Impacts Memory Development in CAR T Cells. Immunity. 2016;44(3):712.
16. Frauwirth KA, Riley JL, Harris MH, et al. The CD28 signaling pathway regulates glucose metabolism. Immunity. 2002;16(6):769-777.
17. Payen VL, Mina E, Van Hée VF, Porporato PE, Sonveaux P. Monocarboxylate transporters in cancer. Mol Metab. 2020;33:48-66.
18. Chen P, Zuo H, Xiong H, et al. Gpr132 sensing of lactate mediates tumor-macrophage interplay to promote breast cancer metastasis. Proc Natl Acad Sci U S A. 2017;114(3):580-585.
19. Colegio OR, Chu NQ, Szabo AL, et al. Functional polarization of tumour-associated macrophages by tumour-derived lactic acid. Nature. 2014;513(7519):559-563.

20. Husain Z, Huang Y, Seth P, and Sukhatme VP. Tumor-derived lactate modifies antitumor immune response: effect on myeloid-derived suppressor cells and NK cells. J Immunol. 2013;191(3):1486-1495.
21. Fischer K, Hoffmann P, Voelkl S, et al. Inhibitory effect of tumor cell-derived lactic acid on human T cells. Blood. 2007;109(9):3812-3819.
22. Uhl FM, Chen S, O'Sullivan D, et al. Metabolic reprogramming of donor T cells enhances graft-versus-leukemia effects in mice and humans. Sci Transl Med. 2020;12(567):eabb8969.
23. Yang L, Chu Z, Liu M. et al. Amino acid metabolism in immune cells: essential regulators of the effector functions, and promising opportunities to enhance cancer immunotherapy. J Hematol Oncol. 2023;16(1):59.
24. Igel P, Dove S, Buschauer A. Histamine H4 receptor agonists. Bioorg Med Chem Lett. 2010;20(24):7191-7199.
25. O'Mahony L, Akdis M, Cezmi AA. Regulation of the immune response and inflammation by histamine and histamine receptors. J Allergy Clin Immunol. 2011;128(6):1153-1162.
26. Noel M, Chasman DI, Mora S, et al. The Inflammation Biomarker GlycA Reflects Plasma N-Glycan Branching. Clin Chem. 2023;69(1):80-87.
27. Otvos JD, Shalaurova I, Wolak-Dinsmore J, et al. GlycA: a composite nuclear magnetic resonance biomarker of systemic inflammation. Clin Chem. 2015;61(5):714-723.
28. Liu Y, Jie X, Nian L, et al. A combination of pre-infusion serum ferritin, CRP and IL-6 predicts outcome in relapsed/refractory multiple myeloma patients treated with CAR-T cells. Front Immunol. 2023;14:1169071.
29. Dall'Olio F, Vanhooren V, Chen CC, Slagboom PE, Wuhrer M, Franceschi C. N-glycomic biomarkers of biological aging and longevity: a link with inflammaging. Ageing Res Rev. 2013;12(2):685-698.

30. Saldova R, Royle L, Radcliffe CM, et al. Ovarian Cancer is Associated with Changes in Glycosylation in Both Acute-Phase Proteins and IgG. Glycobiology. 2007;17(12):1344-1356.

Table 1. Patient and disease characteristics before CAR-T cell therapy

MEDIAN AGE (range)	60.5 (21-70)
GENDER	
Male	33 (75 %)
Female	11 (25 %)
BMI	
<25	15 (34%)
≥25	29 (66%)
ECOG	
0	35 (79.5%)
≥1	9 (20.5%)
DIAGNOSIS	
DLBCL	21 (47.7%)
HGBCL	2 (4.6%)
PMBCL	6 (13.6%)
tFL	15 (34.1%)
BULKY DISEASE	
NA	1 (2.3%)
Yes	28 (63.6%)
No	15 (34.1%)
STAGING	
I-II	12 (27.3%)
III-IV	32 (76.7%)
IPI score	
NA	6 (13.6%)
0-2	23 (52.3%)
≥3	15 (34.1%)
BRIDGING THERAPY	
Chemo-based	16 (36%)
CELLULAR INFUSED PRODUCT	
Axi-cel	24 (55%)
Tisa-cel	20 (45%)
CAR-HEMATOTOX SCORE	
0-1	35 (79.5%)
≥2	9 (20.5%)
CRS	
Yes	38 (86.4%)
No	6 (13.6%)
ICANS	
Yes	14 (31.8%)
No	30 (68.2%)
TOTAL	**44**

Abbreviations: ECOG: Eastern Cooperative Oncology Group performance scale; BMI: body mass index; DLBCL: Diffuse Large B Cell Lymphoma; t-FL: transformed Follicular Lymphoma; HGBCL: High-Grade B Cell Lymphoma; PMBCL: Primary Mediastinal B Cell Lymphoma. IPI: International Prognostic Index. CRS: Cytokine Release Syndrome. ICANS: Immune Cell-Associated Neurotoxicity Syndrome.

Figure Legends

Figure 1. Pre-lymphodepletion (PLD) plasma metabolic differences correlated with anthropometric and clinical parameters collected at PLD time point. Relationships among principal components 1 and 2 (PC1 and PC2) and gender, body mass index (BMI), bridging therapy (BT), Eastern Cooperative Oncology Group performance scale (ECOG), diagnosis, staging, International Prognostic Index (IPI), HEMATOTOX, bulky, Immune Cell-Associated Neurotoxicity Syndrome (ICANS). P-values ($p<0.05$) are calculated by the Kruskal-Wallis test adjusted with Bonferroni correction for multiple comparisons.

Figure 2. Pre-infusion construction of a discriminative model at pre-lymphodepletion (PLD) time point. (A) Spearman *r* coefficient heat maps of principal components 1 and 2 (PC1 and PC2) correlated variables namely triglycerides, lactate dehydrogenase (LDH), fibrinogen, ferritin, and C-reactive protein (CRP) measured at pre-lymphodepletion (PLD) time point. (B) ROC curves of the two models based on the whole set of patients. (C) Orthogonal partial least squares discriminant analysis (OPLS-DA) score plot and (D) the corresponding S-line plot of PLD metabolic profile of patients stratified according to the last follow up available after CAR-T cell infusion (CR, n=13 *vs* PD, n=26).

Figure 3. Post infusion metabolic profile evolution according to the infused product. (A, C, D) Orthogonal partial least squares discriminant analysis (OPLS-DA) for D1, D7, and D30 time points; Statistical parameters of supervised OPLS-DA models for each of the considered time points. R^2X and R^2Y indicate the fraction of variance of the X and Y matrix, respectively. Q^2 is a goodness of prediction parameter representing the portion of the variance in the data predictable by the model. (B) S-line plot related to tisa-cel-treated patients vs those infused with axi-cel at D1 time point.

Figure 4: Post-infusion time-dependent metabolic changes according to the last available follow-up. Orthogonal partial least squares discriminant analysis (OPLS-DA) shows post infusion time-dependent metabolic changes in (A) CR/PR compared to (C) PD patients. (B and D) Volcano

plots (poso(corr) vs. VIP) for the OPLS-DA models. Only the most discriminating metabolites with high VIP values are labelled. Negative poso(corr) values (left) indicate low levels, whereas positive poso(corr) values (right) indicate increased metabolite amount in patients at D30 *vs* D1 time points.

Figure 5. Metabolic profile at D30 time point. (A) Orthogonal partial least squares discriminant analysis (OPLS-DA) for CR patients lasting one year after therapy (stable CR>D30) and those who relapsed within one year (relapsed>D30). (B) S-line plot related to patient group, namely relapsed>D30 compared to stable CR>D30. (C) Fold change comparison of the discriminant metabolites calculated in the comparison of CR patients lasting one year after therapy (stable CR>D30) vs those who relapsed within one year (relapsed>D30). (D) Box-whisker plots showing the significantly discriminant metabolites between relapsed>D30 and stable CR>D30. The x-axis reports the specific metabolite group, and the y-axis the normalized peak intensity. P-values ($p<0.05$) are calculated by unpaired t-test.

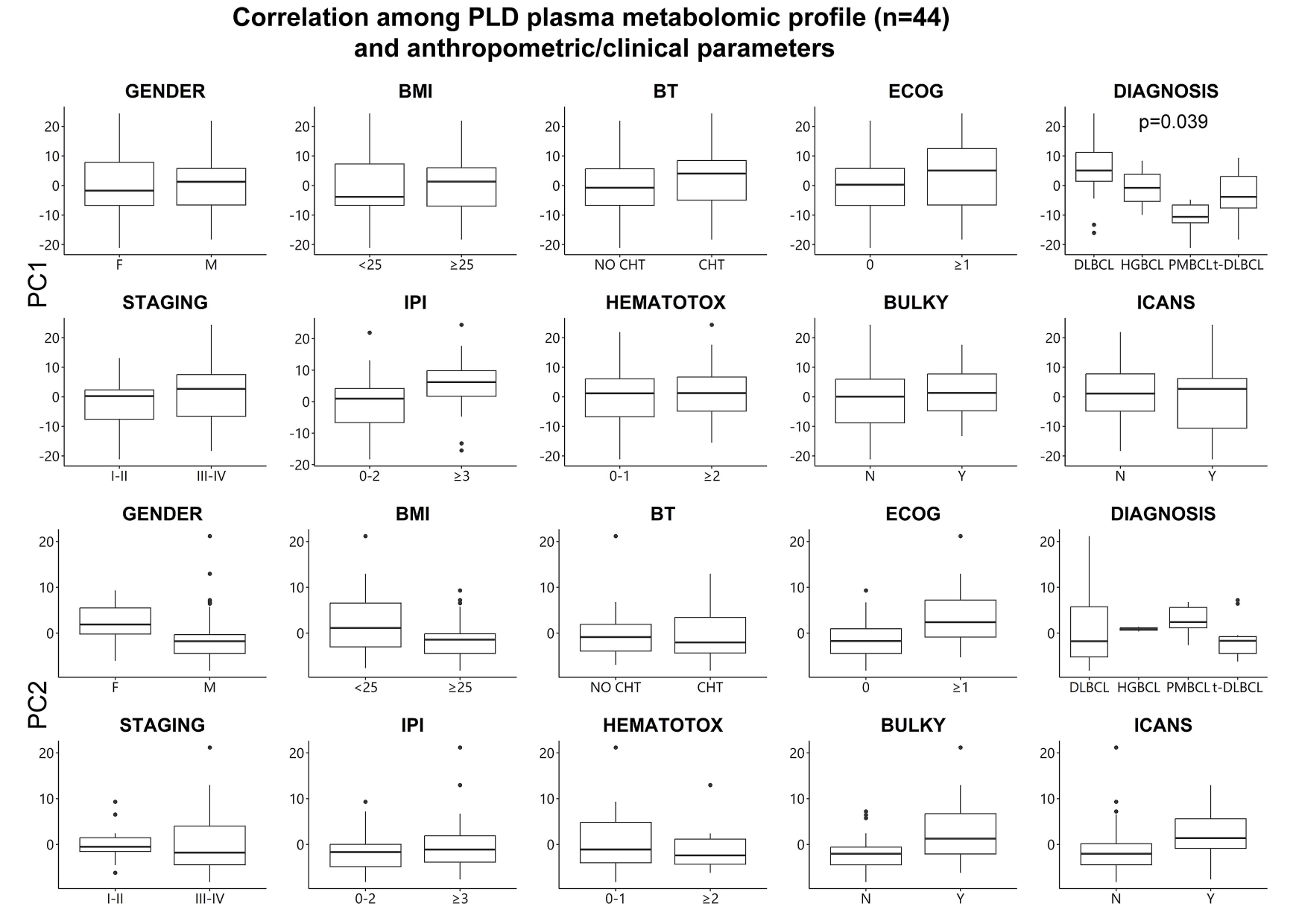
Correlation among PLD plasma metabolomic profile (n=44)
and anthropometric/clinical parameters
PC1
PC2
GENDER
F
M
BMI
<25
≥25
BT
NO CHT
CHT
ECOG
0
≥1
DIAGNOSIS
p=0.039
DLBCL
HGBCL
PMBCL
t-DLBCL
STAGING
I-II
III-IV
IPI
0-2
≥3
HEMATOTOX
0-1
≥2
BULKY
N
Y
ICANS
N
Y

Construction of discriminative model at PLD time point

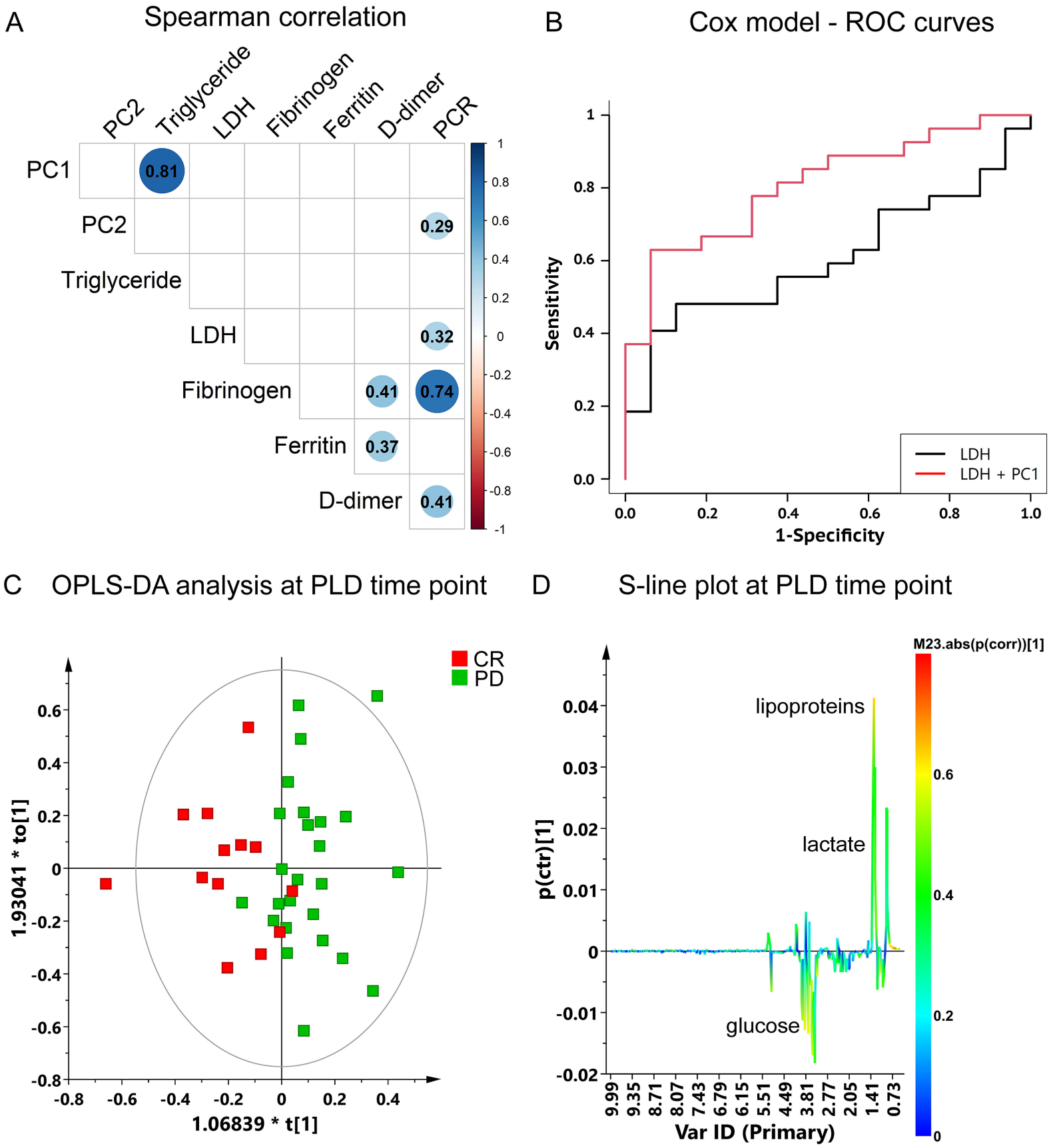

Post infusion metabolic profile evolution according to the infused product

A

OPLS-DA at D1 N=22

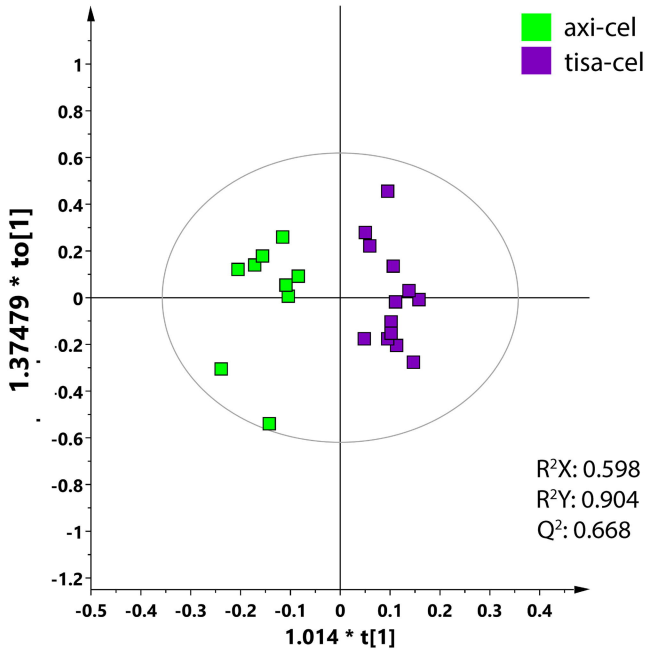

B

S-line plot: tisa-cel vs axi-cel

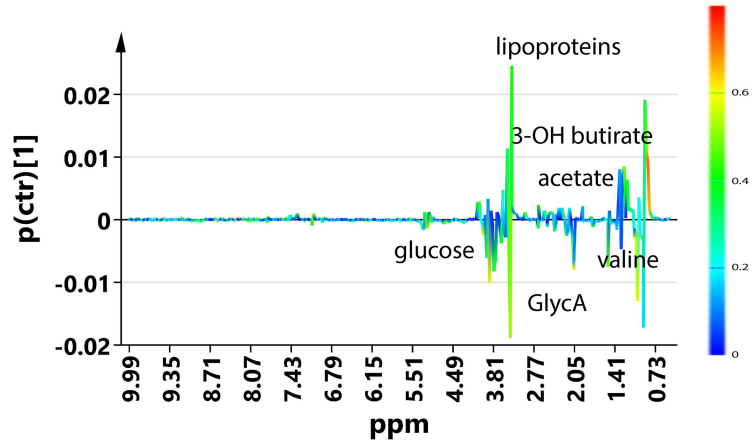

C

OPLS-DA at D7 N=22

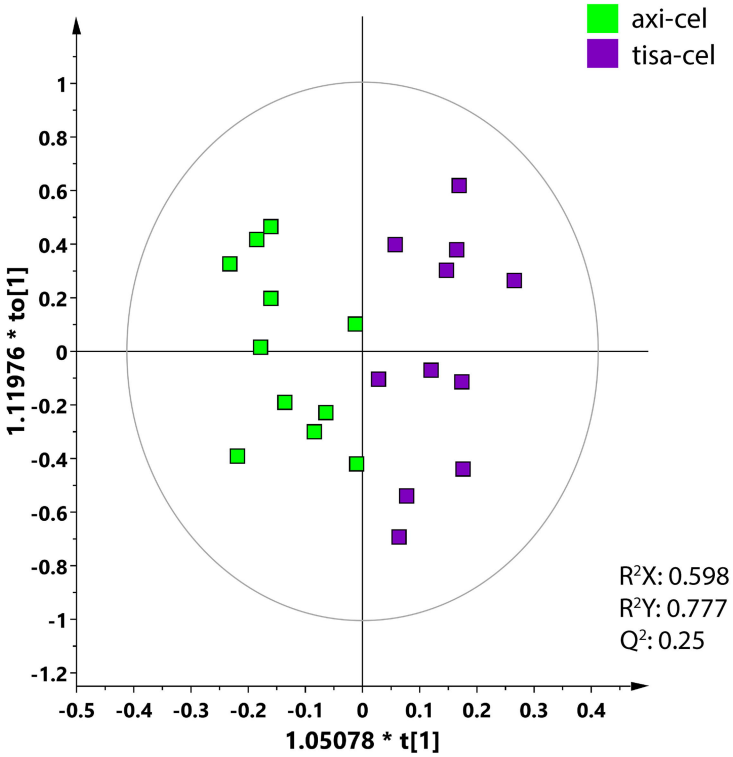

D

OPLS-DA at D30 N=22

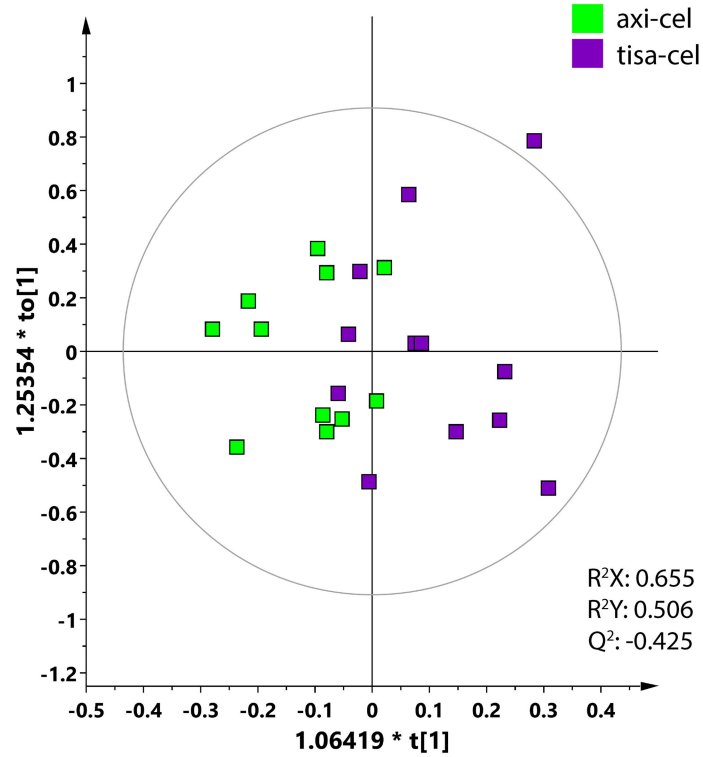

Time-dependent post infusion metabolic changes according to the last available follow-up

A CR/PR patients

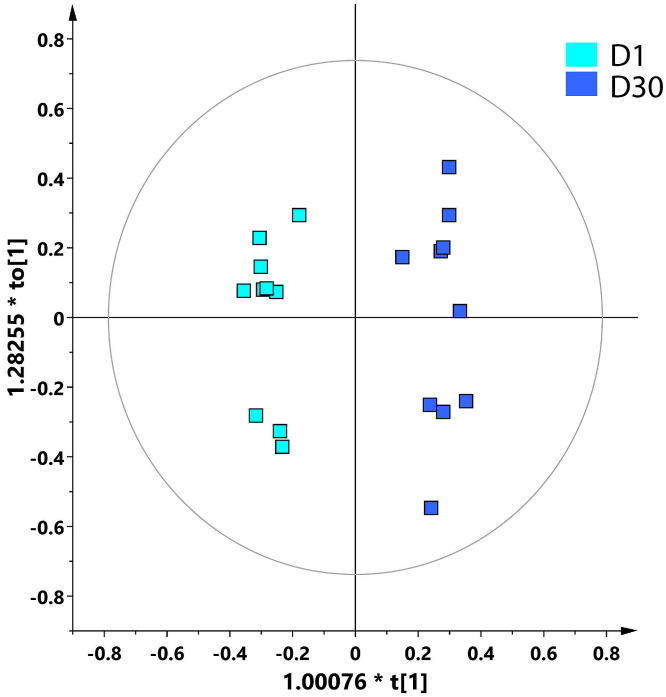

B CR/PR patients

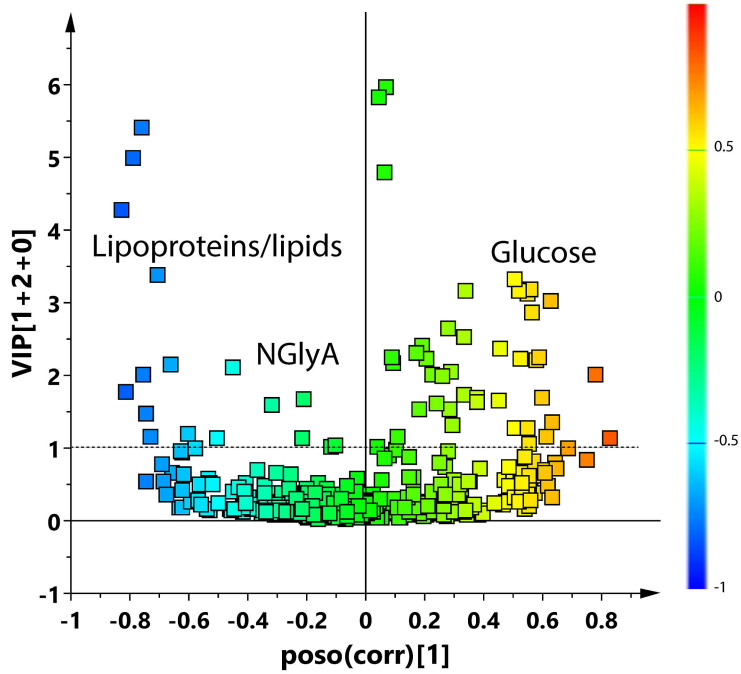

C PD patients

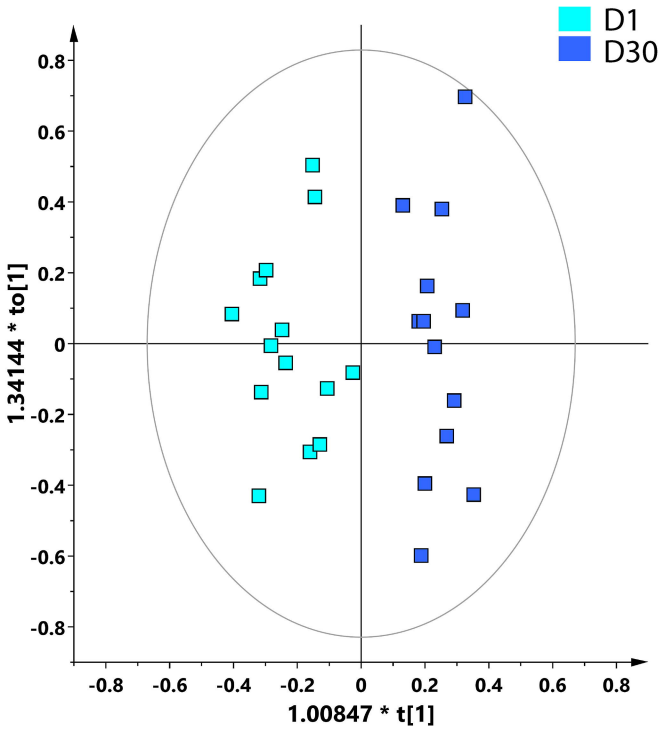

D PD patients

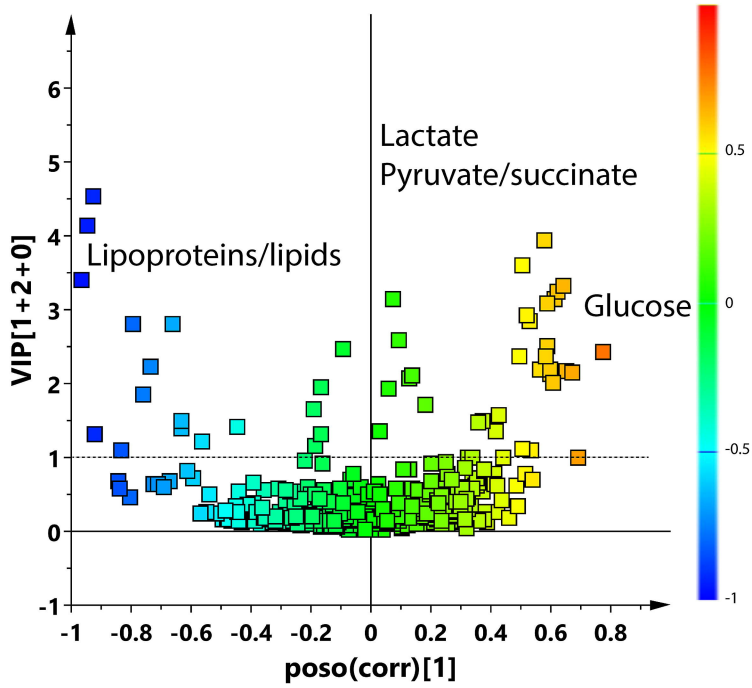

Metabolic profile at D30 time point

A

OPLS-DA analysis at D30
N=14

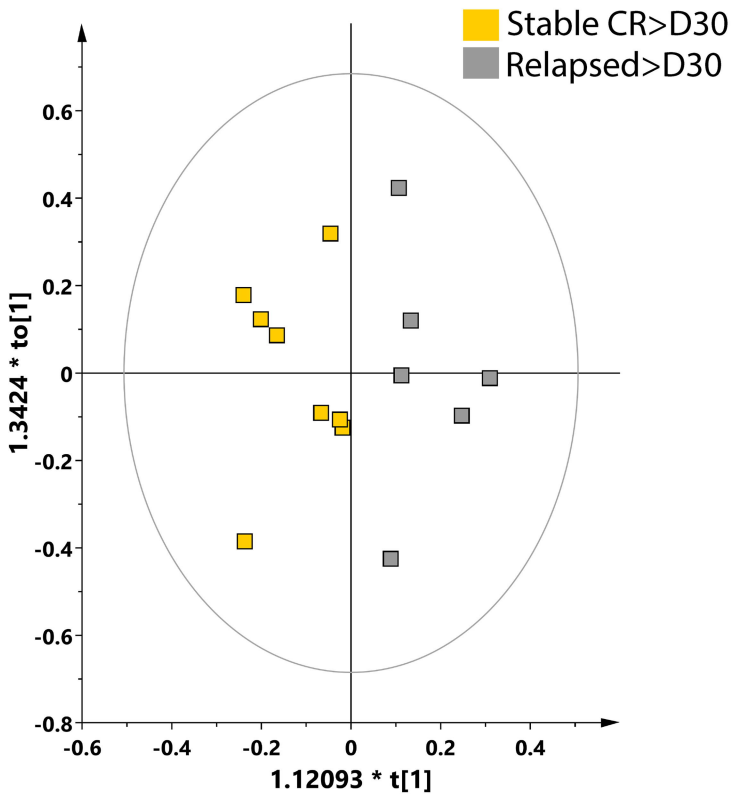

B

S-line plot:
Relapsed >D30 vs Stable CR >D30

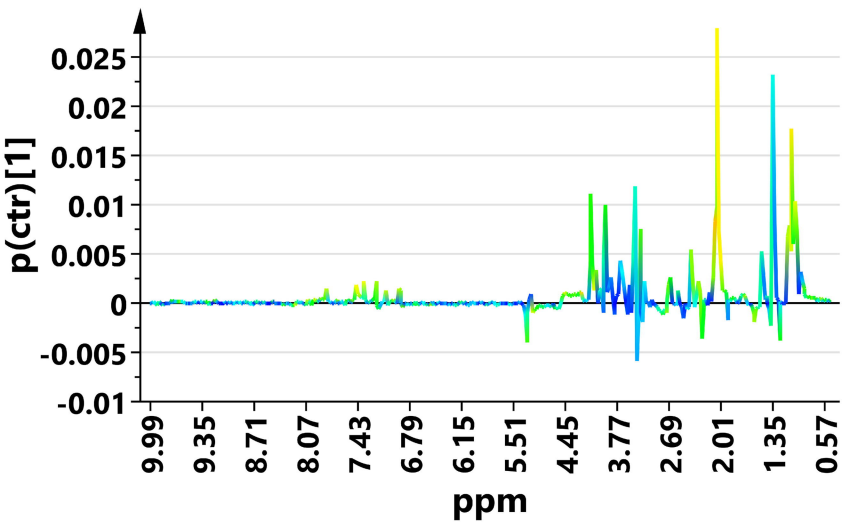

C

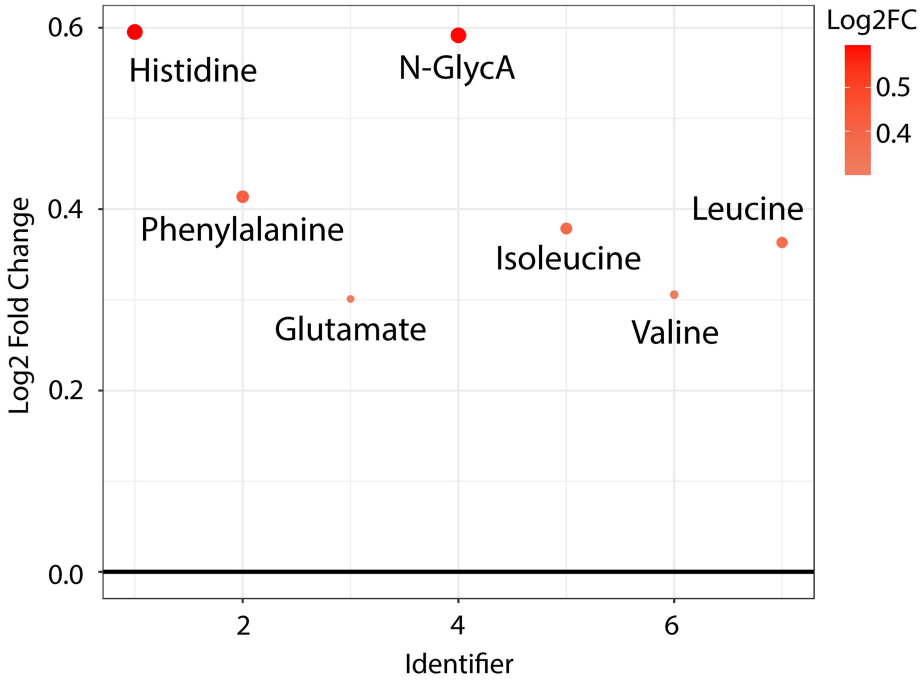

D

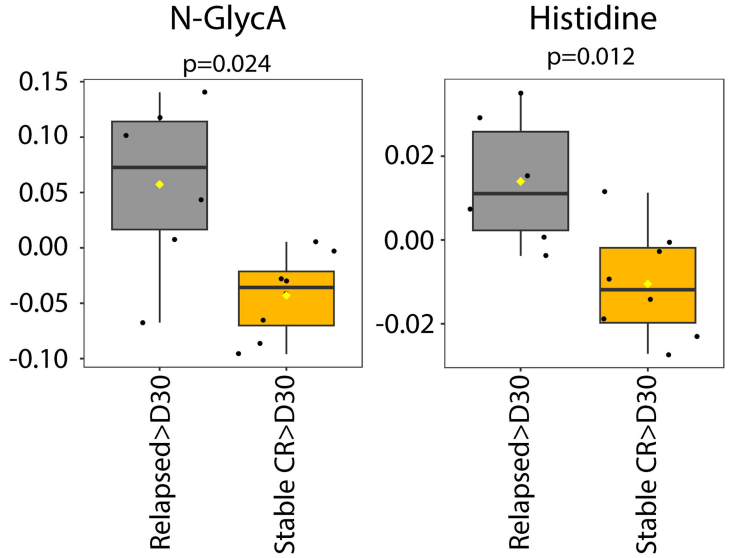

Supplementary Methods

NMR measurement and data processing

Plasma samples were thawed at room temperature and 5 mm NMR tubes were prepared for NMR measurement by adding 200 µL of sample with 400 µL of saline buffer solution at pH 7.4 (NaCl 0.9%, 50 mM of sodium phosphate buffer in D_2O containing trimethylsilyl propionic-2,2,3,3-d4 acid sodium salt, TSP). ^{1}H-NMR spectra for all plasma samples were recorded on a Bruker Avance III NMR spectrometer (Bruker, Ettlingen, Germany), at a frequency of 600.13 MHz for ^{1}H observation, equipped with a TCI cryoprobe (Triple Resonance inverse Cryoprobe), and incorporating a z-axis gradient coil and automatic tuning-matching. Experiments were carried out at 300 K in automation mode using a Bruker Automatic Sample Changer, which interfaced with the software IconNMR version 5.0.9. For each sample, a standard 1D-^{1}H Carr-Purcell-Meiboom-Gill (1D-CPMG) experiment (with suppression of water resonance) was performed to filter out signals belonging to proteins and other macromolecules, thus obtaining spectra primarily comprising signals from metabolites and small molecules.[1,2] Free induction decays (with a FID size of 64 K data points) were collected by averaging 128 transients, 16 dummy scans, a 5 s relaxation delay, 12,019.230 Hz (20.0276 ppm) spectral width, an acquisition time of 1.36 s, 1.2 ms delay (d20, fixed echo time to allow elimination of J modulation effects according to the Bruker pulse program code, with a loop of 126 cycles for T2 filter), obtaining a total value of total spin-spin relaxation delay of 302.4 ms. The resulting FIDs were multiplied by an exponential weighting function corresponding to a line broadening of 0.3 Hz before Fourier transformation, automated phasing, and baseline correction. 2D NMR spectra (^{1}H Jres, ^{1}H-^{1}H COSY, ^{1}H-^{13}C HSQC, and ^{1}H-^{13}C HMBC) were also randomly acquired for assignment purposes, and metabolites identified according to the public database Human metabolome database and ChenomX NMR Suite 8 (ChenomX Inc., Edmonton, Canada) software, together with a comparison with other published data.[2,3]

The NMR spectra were processed using Topspin 3.6.1 and Amix 3.9.13 (Bruker, Biospin, Italy), both for simultaneous visual inspection and the successive bucketing process for multivariate statistical analyses. The entire NMR spectrum (in the range of 10.0–0.5 ppm) was segmented in fixed rectangular buckets 0.02 ppm in width and successively integrated. Chemical shifts were referenced to TSP as an internal standard (δH 0.00 ppm) and the spectral region between 4.90-4.50 ppm was discarded to avoid the effects of water suppression. Moreover, a total of other six spectral regions were not taken into consideration, due to the residual peaks of solvents and identification of the anticoagulant ethylenediaminetetraacetic acid (EDTA) between 4.06-4.00, 3.70-3.57, 3.30-3.00, 2.77-2.70, 2.60-2.55 and 1.20-1.15 ppm. Centering, normalization to a constant sum, and the Pareto scaling were applied to the bucketed NMR data to improve the performance of downstream statistical analyses.[4]

Plasma profile of circulating N-glycans

Plasma samples were obtained from an independent cohort of 20 patients who were in CR/PR on the basis of the D30 PET/TC scans. Circulating plasma profile of ten N-glycans was assessed at D30 time point by using "DNA Sequencer Adapted-Fluorophore Assisted Carbohydrate Electrophoresis" (DSA-FACE), as previously described[5]. Briefly, 2 ul of plasma were treated with a denaturing buffer, labeled with 8-amino-1,3,6-pyrenetrisulfonic acid (APTS), desialylated and read-out with a microcapillary electrophoresis on an automated Sanger sequencing platform to obtain the corresponding peaks profile. The relative height of each peak, which represents the relative concentration of the oligosaccharide structures, was calculated as the ratio between the height of the peak and the sum of the heights of the ten peaks (**Supplementary Fig. S4**). Finally, the GlycoAge[6] score has been calculated as the log ratio of peak1 (NGA2F) and peak6 (NA2F) (**Supplementary Fig. S4).**

References

1. Vignoli A, Ghini V, Meoni G, et al. High-throughput metabolomics by 1D NMR. Angewandte Chemie International Edition. 2019;58(4):968-994.
2. Del Coco L, Greco M, Inguscio A, et al. Blood Metabolite Profiling of Antarctic Expedition Members: An ^{1}H NMR Spectroscopy-Based Study. International Journal of Molecular Sciences. 2023;24(9):8459.
3. Foxall PJ, Spraul M, Farrant RD, Lindon LC, Neild GH, Nicholson JK. 750 MHz 1H-NMR spectroscopy of human blood plasma. J Pharm Biomed Anal. 1993;11(4-5):267-276.
4. van den Berg RA, Hoefsloot HC, Westerhuis JA, Smilde AK, van der Werf MJ. Centering, scaling, and transformations: improving the biological information content of metabolomics data. BMC Genomics. 2006;7:142.
5. Vanhooren V, Laroy W, Libert C, Chen C. N-glycan profiling in the study of human aging. Biogerontology. 2008;9(5):351-356.
6. Vanhooren V, Dewaele S, Libert C, et al. Serum N-glycan profile shift during human ageing. Exp. Gerontol. 2010; 45(10):738-743.

Supplementary Figures

Figure S1. A) Flow chart of the study population. (B) Representative ^{1}H NMR spectrum of metabolites obtained from a plasma sample. BCAA: valine, leucine, isoleucine; N-GlycA: N-acetyl groups of glycoproteins; *: EDTA.

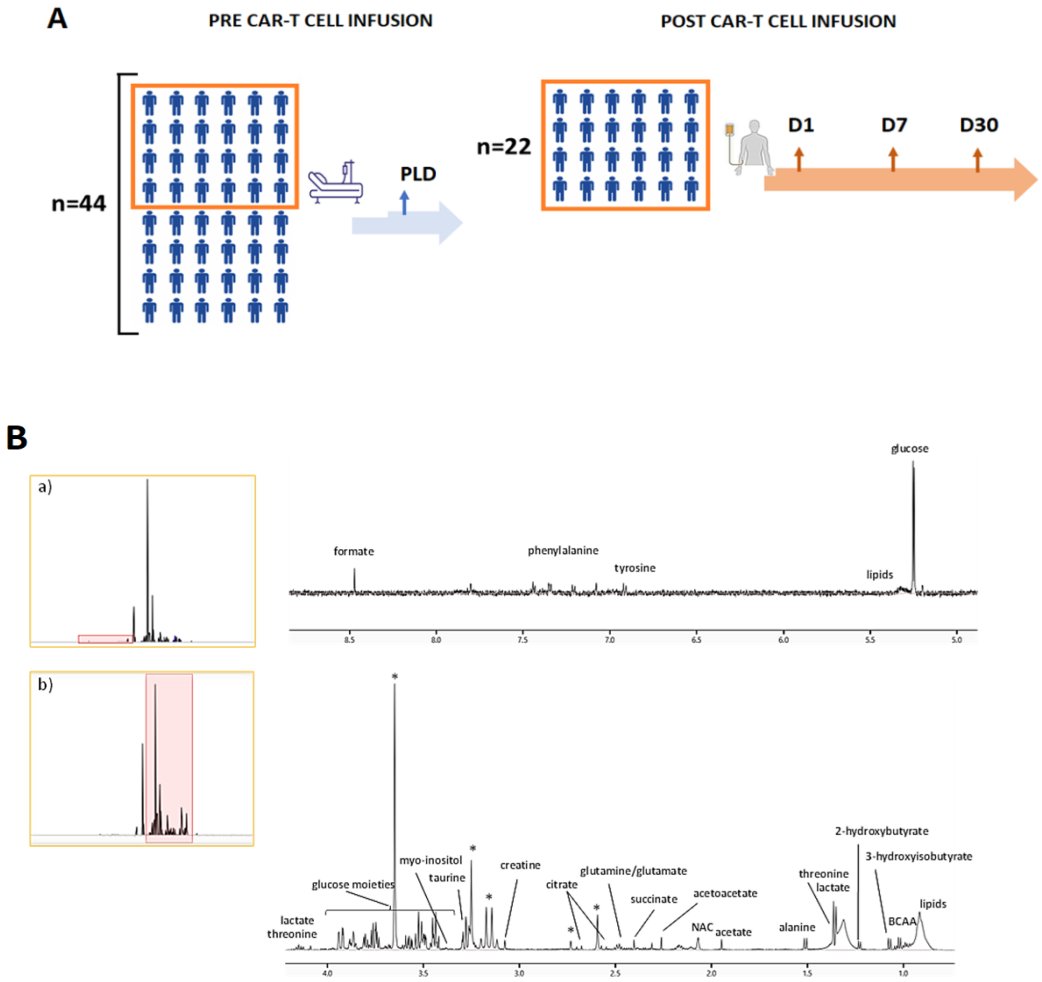

Figure S2. Principal component analysis (PCA) obtained considering patients at PLD time point. (A) Scree plot reporting the percentage of variance explained by each component in the model. (B) Principal component 1 and 2 (PC1 vs PC2) loading plot explaining the contribution of the loadings for the first two components. (C) Box-whisker plot distribution of discriminant metabolites between patients stratified according to the last available follow up (CR, n=13, PD, n=26, PR, n=3).

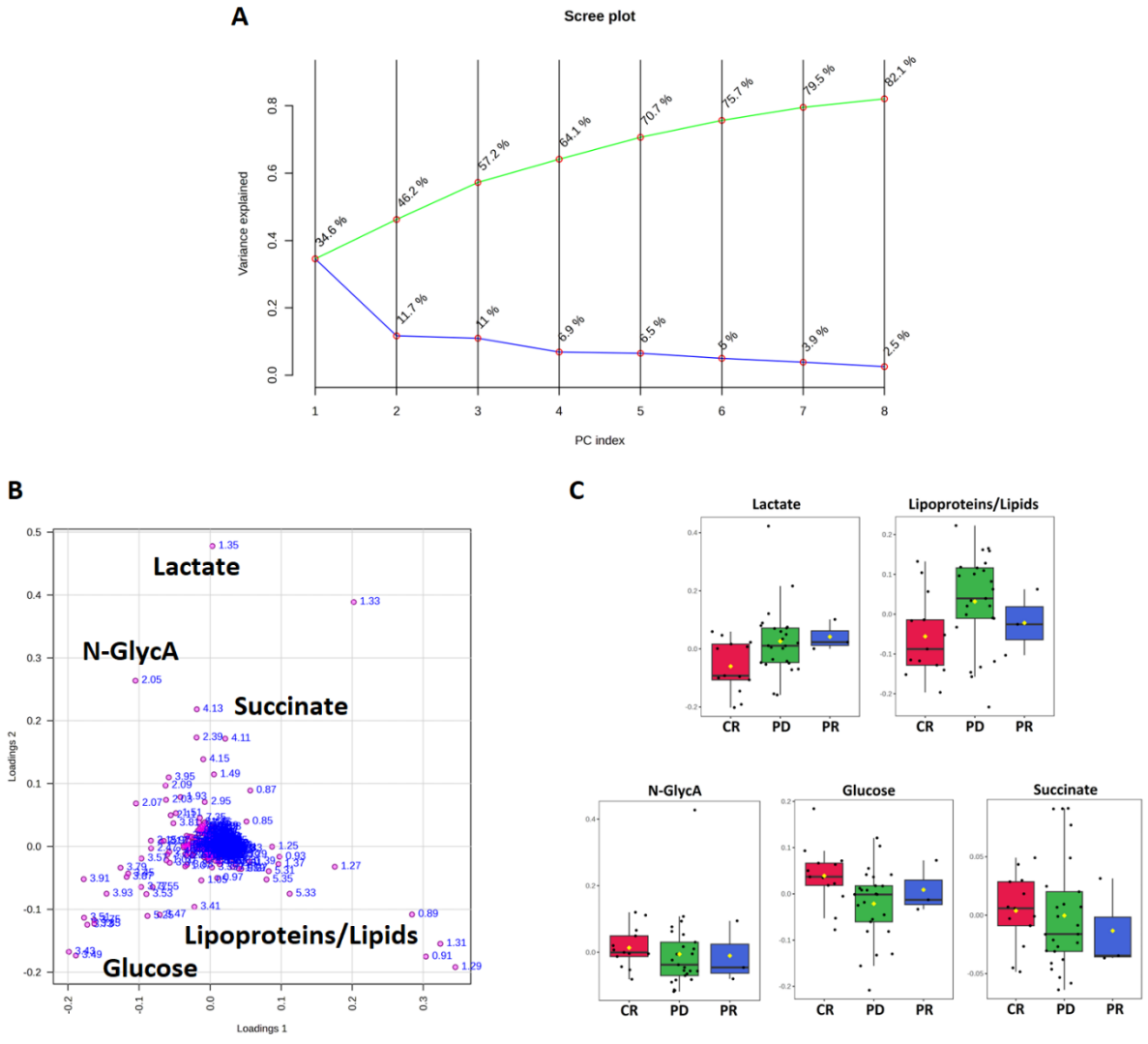

Figure S3. Orthogonal partial least squares discriminant analysis (OPLS-DA) for pre-lymphodepletion (PLD) time point in patients treated with axi-cel and tisa-cel.

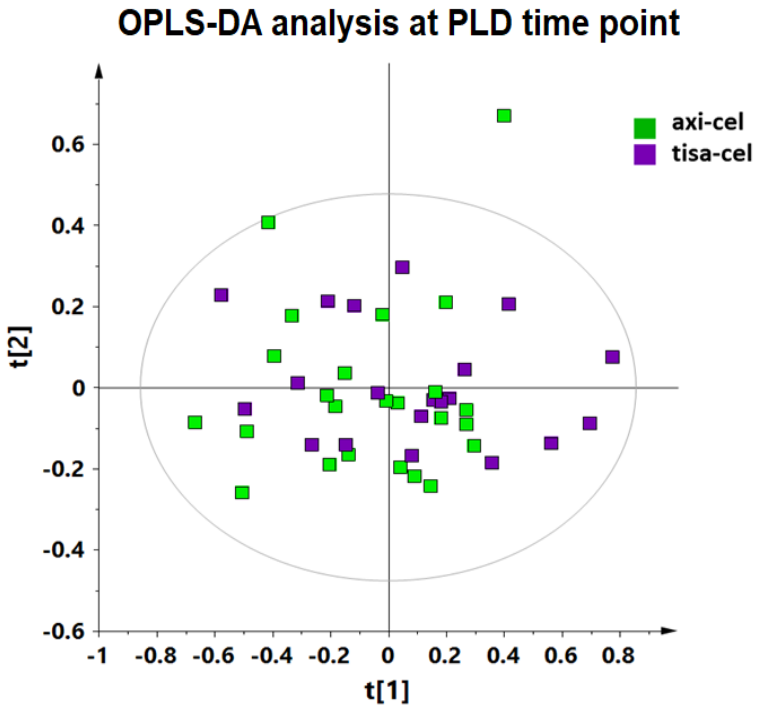

Figure S4. Circulating plasma profile of N-glycans. Ten N-glycans were assessed at D30 time point by using "DNA Sequencer Adapted-Fluorophore Assisted Carbohydrate Electrophoresis" (DSA-FACE). The Log of the ratio of the relative abundance of peak 1 (NGA2F) and peak 6 (NA2F) is the GlycoAge Test that is applied between CR patients lasting one year after therapy (CR>D30) (n=12) and those who relapsed within one year (relapsed>D30) (n=8).

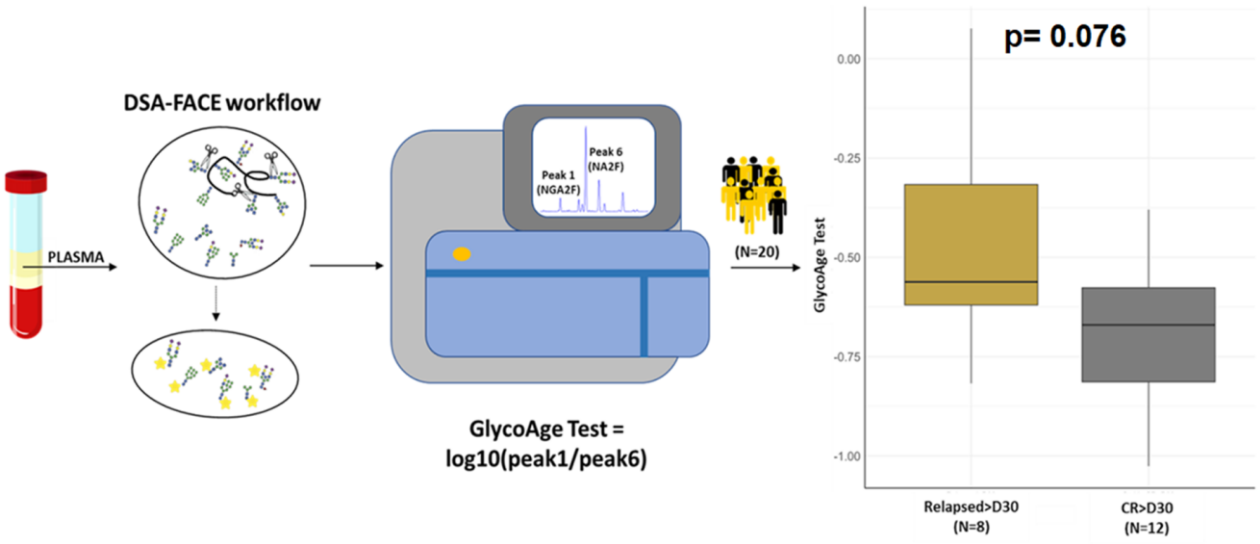

Table S1. Chemical shifts (δ) and assignments of metabolites resonances in the ^{1}H NMR spectra of the detected human plasma

Metabolites	**^{1}H NMR chemical shift (δ, ppm)**
2-hydroxybutyrate	1.13(d); 2.55(m)
3-hydroxybutyrate	1.20(d); 2.31(m)
Acetate	1.92(s)
Acetoacetate	2.22(s)
Alanine	1.48(d); 3.78(q)
Citrate	2.52(d); 2.69(d)
Creatine	3.04(s); 3.93(s)
Formate	8.46(s)
Glutamate	2.10(m); 2.35(m); 3.78(t)
Glutamine	2.14(m); 2.46(m)*; 3.78(t)
Histidine	3.14(m); 3.25(m); 3.99(m); 7.09(s); 7.85(s)
Isoleucine	0.94(t); 1.01(d); 1.26(m); 1.46(m); 1.98(m); 3.67(d)
Lactate	1.33(d); 4.12(q)
Leucine	0.96(d); 0.97(d); 1.70(m); 3.75(m)
Lipoproteins (LDL, VLDL)/lipids	0.87(t); 0.93(m); 1.25(m); 1.29(m); 5.30-5.35(m)
myo-Inositol	3.25(t); 3.61(dd); 4.07(t)
NAC	2.04(s)
Phenylalanine	3.13(m); 3.28(m); 4.00(m); 7.33(d); 7.38(t); 7.43(m)
Pyruvate	2.37 (s)
Succinate	2.41(s)
Tyrosine	3.06(m); 3.20(m); 3.94(m); 6.92(d); 7.20(d)
Taurine	3.25(t); 3.43(t)
Threonine	1.33(d); 3.59(d); 4.25(m)
Tyrosine	3.06(m); 3.20(m); 3.94(m); 6.92(d); 7.20(d)
Valine	0.99(d); 1.04(d); 2.28(m); 3.61(d)
α-Glucose	3.42(t); 3.54(dd); 3.71(t); 3.74(m); 3.84(m); 5.24(d)
β-Glucose	3.25(dd); 3.41(t); 3.46(m); 3.49(t); 3.72(dd); 3.90(dd); 4.65(d)

Table S2. List of discriminating chemical descriptors (variables) with corresponding correlation coefficient (pcorr), and variable importance on the projection (VIP) for PD *vs* CR patients OPLS-DA model reported in Figure 2D.

Metabolites (Var ID)	VIP [1+1+0]	p(corr) [1]
Glucose (5.25 ppm)	1.44377	1.06031
Lactate (1.33 ppm)	5.61972	0.598393
Lipoproteins (0.89 ppm)	5.23888	2.38028

Table S3. List of discriminating chemical descriptors (variables) with corresponding correlation coefficient (pcorr), and variable importance on the projection (VIP) for tisa-cel *vs* axi-cel OPLS-DA model reported in Figure 3B.

Metabolites (Var ID)	VIP [1+2+0]	p(corr) [1]
Glucose (5.25 ppm)	1.65228	0.0846376
N-GlycA (2.05 ppm)	3.0474	-0.610006
Acetate (1.93 ppm)	1.08554	0.141068
3-OH butyrate (1.21 ppm)	2.16289	0.359449
Valine (1.01 ppm)	4.95483	-0.170613
Lipoproteins (0.89 ppm)	4.17727	0.351978

Table S4. Significance of the Fold change comparison of the discriminant metabolites between CR patients lasting one year after therapy (stable CR>D30) and those who relapsed within one year (relapsed>D30), derived from the unpaired t-test.

Metabolite	**Fold Change**	**Log_2(FC)**	**p-value**
Histidine	1.5108	0.59535	0.012
N-GlycA	1.507	0.59169	0.024
Phenylalanine	1.3321	0.41372	0.133
Isoleucine	1.3001	0.3786	0.130
Leucine	1.2863	0.36323	0.143
Valine	1.236	0.3057	0.07
Glutamate	1.232	0.30098	0.2165